Nonlinear Analysis: Modelling and Control, Vol. 29, No. 3, 509–527
https://doi.org/10.15388/namc.2024.29.34884

Synchronization of delayed stochastic reaction–diffusion Hopfield neural networks via sliding mode control*

Xiao Liang[a,1], **Yiyi Yang**[a], **Ruili Wang**[b], **Jiangtao Chen**[c],

[a]School of Mathematics and System Science,
Shandong University of Science and Technology,
Qingdao, China, 266590
mathlx@163.com

[b]Institute of Applied Physics and Computational Mathematics,
Beijing, China, 100094

[c]China Aerodynamics Research and Development Center,
Mianyang, China, 621000

Received: February 12, 2023 / **Revised:** November 9, 2023 / **Published online:** March 23, 2024

Abstract. Synchronization of stochastic reaction–diffusion Hopfield neural networks with s-delays via sliding mode control is investigated in this article. To begin with, we choose suitable functional space for state variables, then the system is transformed into a functional differential equation in an infinite-dimensional Hilbert space by using appropriate functional analysis technique. Based on above preliminary preparation, sliding mode control (SMC) is constructed to drive the error trajectory into the designed switching surface. Specifically, the switching surface is constructed as linear combination of state variables, which is related to control gains. Then novel SMC law is designed which involving delay, reaction diffusion term, and reaching law. Furthermore, the criterion of mean-square exponential synchronization for stochastic delayed reaction–diffusion Hopfield neural networks with s-delays is given in the form of matrix form. This criterion is less restrictive and easy to check in computer. Meanwhile, a different novel Lyapunov–Krasovskii functional (LKF) mixed with Itô's formula, Young inequality, Hanalay inequality is employed in this proof procedure. At last, a numerical example is presented to validate the availability of theoretical result. The simulation is based on the finite difference method, and numerical result coincides with the theoretical result proposed.

Keywords: Lyapunov–Krasovskii functional, synchronization, sliding mode control, Wiener process, distributed systems.

*The work was supported by Shandong Provincial Natural Science Foundation (No. ZR2021MA056), National Numerical Wind-Tunnel (No. NNW2019ZT7-A13) and Joint Funds of the National Natural Science Foundation of China (No. U2230208).

[1]Corresponding author.

© 2024 The Author(s). Published by Vilnius University Press
This is an Open Access article distributed under the terms of the Creative Commons Attribution Licence, which permits unrestricted use, distribution, and reproduction in any medium, provided the original author and source are credited.

1 Introduction

Synchronization generally means that two systems with different initial conditions are forced to achieve identical dynamics after finite time under appropriate control law [18]. As an important collective behavior, synchronization of Hopfield neural networks (HNNs) becomes a hot research topic in recent decades due to its potential applications in secure communications, information processing, and distributed computation [4, 10, 11, 14, 19, 23–25,30]. As we all know, the original controlled models of HNNs are described through nonlinear ordinary differential equations. They are just the approximations of real world, the following vital factors are neglected in the standard HNNs.

To begin with, a delay is inevitably encountered in implementation of neural networks (NNs) through very large scale integration (VLSI) system due to finite speed of switching and transmission of signals [4, 10, 11, 24, 25, 27, 28, 30]. Two main types of delays are investigated in published work of delayed HNNs. Some scholars assume that delay is a constant number in operation of HNNs. Mathematically, they focus on HNNs with discrete delays $f_i(u_i(t-\tau_i))$, $i = 1, 2, \dots, n$, where f_i, $i = 1, 2, \dots, n$, are the activation functions of HNNs [30]. Other scholars notice that NNs have spatial nature since the presence of a multitude of parallel pathways. In this case, it is reasonable to study the HNNs with distributed delays $\int_{-\tau_i}^{0} f_i(u_i(t+\theta))k_i(\theta)\,\mathrm{d}\theta$, k_i are kernel functions [19, 27, 28]. Both of them can be included in the s-delays $\int_{-\tau_i}^{0} f_i(u_i(t+\theta))\,\mathrm{d}\kappa_i(\theta)$ with $\mathrm{d}\kappa_i$ satisfying Lebesgue–Stieltjes measure [9]. So the HNNs with s-delay is much more general than other type of delayed HNNs, whether in mathematics or physics.

Meanwhile, diffusion effect cannot be ignored in HNNs when electrons move in an asymmetrical electromagnetic field [8–11, 14, 19, 24, 28]. The diffusion operator with convection-advection term rather than the Laplacian Δ operator is explored in this article to describe the diffusion phenomenon. The diffusion operator with convection-advection term can be degenerated to the Laplacian operator when the diffusion coefficient matrix is chosen to be an identity matrix. Furthermore, from physical viewpoint, diffusion operator with convection-advection term means that the particle diffuses heterogeneously, while Laplacian operator means that the particle diffuses homogenously. So diffusion operator with convection-advection term is much more general than Δ operator [24, 25].

Furthermore, it is particularly worth mentioning that the synaptic transmission is a noisy process brought on by random fluctuations from the release of neurotransmitters and other probabilistic causes in real nerve systems [4, 14, 19, 27–29]. Wiener process used in this paper is an efficient and common tool in characterising random external disturbance.

We can infer from above discussion that the predictability of HNNs will be significantly improved if s-delays, reaction diffusion term, and stochastic factors are taken into consideration. However, delays, reaction diffusion term, and Wiener processes are also sources of bifurcation, chaos, and instability, which are harmful to the system in the practical design. In view of this disadvantage, the scholars might hesitate to adopt the stochastic reaction diffusion Hopfield neural networks (SRDHNNs) with s-delays. Therefore, synchronization will be a critical technique if we want to make the best use of the advantage of SRDHNNs with s-delays and hedge their bets. Unfortunately, there is still no result on synchronization of SRDHNNs with s-delays due to complex structure. The difficulty of tackling synchronization of SRDHNNs with s-delays will be magnified by simultaneous existence of s-delay, reaction–diffusion term, and Wiener process. This is one of the motivation of this article.

In order to track the desired trajectory in the controlled system, we are inclined to use the sliding mode control(SMC) technique to reduce the tracking error for SRDHNNs with s-delays since it is an effective discontinuous control strategy. It has numerous attractive features such as fast response, good transient performance, and robustness subject to uncertainties and external disturbance. It can even stabilize the complex nonlinear systems, which are difficult to stabilize by continuous control [6, 7, 12, 17, 22]. After checking the published papers, we find there is still little paper involving synchronization of HNNs via SMC. Integral SMC approach is used to investigate the synchronization of nonidentical chaotic neural networks with constant delays in [5], equivalent control is constructed based on integral sliding manifold. However, random disturbance and diffusion effect is missed in that model. SMC based on equivalent control is also utilized in control of deterministic reaction diffusion Hopfield neural networks in [7]. But his methodology will be failed if Wiener process is added in the system of [7]. As far as we know, synchronization of SRDHNNs with s-delays via SMC has not been studied, which is another motivation of this article. The main contribution of this paper is listed in the following terms.

- (i) Choosing the right functional space for state variables is a critical step toward its analysis. The study of synchronization of delayed SRDHNNs is more compact, convenient, and concise when it is carried out on the abstract Hilbert space.
- (ii) Most existing literatures related to synchronization of distributed system via SMC are concentrated on relatively simple, linear, and low-dimensional reaction–diffusion system derived from biological or chemical field. It is a challenge to use SMC to tackle SRDHNNs with s-delays, which are complex and high-dimensional nonlinear dynamical systems. To the best of knowledge, there is no published result on this field yet.
- (iii) One of the trouble lies in how to deal with the reaction–diffusion term in convection–advection form when it comes to the application of SMC to delayed SRDHNNs. This object is solved by implementing semipositive definite assumption of related matrix, and deduction is based on the Gauss formula and Kronecker product.
- (iv) Two novel Lyapunov–Krasovskii functionals (LKFs) are applied in the proof procedures. Both of them are trickly constructed, which is related to the coefficients of switching surface. These LKFs can surmount the difficulty due to coupleness of delay, reaction–diffusion term, and Wiener process. By the way, appropriate bound for noise intensity function is utilized to restrain the impact of noise. The synchronization criterion is given in the form of matrix norm and can be easily checked in computer.
- (v) The program for simulation is written by ourselves. After checking the published paper in the SMC of distributed systems,we found that there is still no software

for synchronization of SRDHNNs with s-delays. It becomes one of our task to develop a software to simulate these objects. The Runge–Kutta–Chebyshev scheme is used to deal with time, second-order center difference scheme is utilized to cope with the space, and Euler–Maruyama formula is used to solve Wiener process.

The rest of this article is organized as follows. The preliminaries and notations are presented in Section 2. The switching surface and control law is designed in Section 3. In Section 4, the synchronization of delayed SRDHNNs under SMC is discussed. Section 5 provides a numerical example to validate the efficiency of theoretical result. The conclusion is drawn and future direction is pointed out in Section 6.

2 Nomenclatures and preliminaries

We begin with a motivational preview on some notations, definitions, and inequalities, which will arise later on the paper.

- $(\Omega, \mathcal{F}, \mathsf{P})$ represents a complete probability space with filtration $\{\mathcal{F}_t\}_{t\geqslant 0}$ satisfying the usual conditions, where Ω is the basic event space, $\mathcal{F}$ is the σ-algebra of sample space, P is the probability measure;
- E is the expectation operator with respect to P;
- $W = (W_1, W_2, \dots, W_m)$ is a m-dimensional mean-zero standard Wiener process defined on $(\Omega, \mathcal{F}, \mathsf{P})$ with independent components;
- For $A \in \mathbb{R}^{n\times n}$, $\det(A)$ denotes the determinant of A;
- For $A \in \mathbb{R}^{n\times n}$, $A > 0$ means that A is a positive definite matrix;
- If $A \in \mathbb{R}^{n\times n}$ and $A^{\mathrm{T}} = A$, $\lambda_M(A)$ denotes the largest eigenvalue of A;
- For $A \in \mathbb{R}^{n\times n}$ and $A^{\mathrm{T}} = A$, $\lambda_m(A)$ denotes the smallest eigenvalue of A;
- E denotes the identity matrix of $\mathbb{R}^{n\times n}$;
- Frobenius norm of $A \in \mathbb{R}^{m\times n}$ is defined as $\|A\|_F = (\mathrm{tr}(A^{\mathrm{T}}A))^{1/2}$;
- For $A = (a_{ij})_{m\times n}$, $B = (b_{ij})_{m\times n}$, $A \circ B = (a_{ij}b_{ij})_{m\times n}$ is called the Hadmard product of A and B [13];
- $\boldsymbol{u}(\cdot)_t$ denotes the restriction of $\boldsymbol{u}(\cdot)$ to the interval $[t-r,\, t]$ translated to $[-r, 0]$. For all $s \in [-r, 0]$, $\boldsymbol{u}_t(s) = \boldsymbol{u}(t+s)$;
- $L^2(\mathcal{O})$ stands for the space of square-integrable functions on $\mathcal{O}$, it becomes a Hilbert space when equipped with the square norm $|\cdot|_{L^2(\mathcal{O})}$ on $\mathcal{O}$;
- $U = \{L^2(\mathcal{O})\}^n$, it becomes a Hilbert space when equipped with the usual inner product $(\boldsymbol{u}, \boldsymbol{v}), \boldsymbol{u}, \boldsymbol{v} \in U$ and the corresponding norm is $\|\boldsymbol{u}\| = \sqrt{(\boldsymbol{u}, \boldsymbol{u})}$;
- $H^k(\mathcal{O})$ is the space of function u in $L^2(\mathcal{O})$ whose distribution derivative of order $\leqslant k$ is in $L^2(\mathcal{O})$;
- $C([-r, 0], U)$ is the Banach space of all continuous functionals from $[-r, 0]$ into U with the sup-norm $\|\boldsymbol{\varphi}\|_C = \sup_{-r\leqslant s\leqslant 0} \|\boldsymbol{\varphi}(s)\|$;
- $\mathfrak{L}^2_{\mathcal{F}_0}([-r, 0]; U)$ denotes the space of all $\mathcal{F}_0$-measurable $C([-r, 0]; U)$-valued random variable, which satisfies $\sup_{-r\leqslant s\leqslant 0} \mathsf{E}\|\boldsymbol{\varphi}(s)\|^2 < \infty$.

The response system of delayed SRDHNNs under adiabatic boundary condition is expressed in the following form:

$$\begin{aligned} \mathrm{d}\boldsymbol{u} &= \left(\nabla\cdot\big(D(\boldsymbol{x})\circ\nabla\boldsymbol{u}\big) - \boldsymbol{A}\boldsymbol{u} + \boldsymbol{C}\boldsymbol{f}\left(\int_{-r}^{0}\boldsymbol{u}(t+s,\,\boldsymbol{x})\,\mathrm{d}\eta(s)\right) + \boldsymbol{I}\right)\mathrm{d}t, \\ \frac{\partial\boldsymbol{u}}{\partial\nu}&(t,\boldsymbol{x}) = 0, \quad t\geqslant 0,\ \boldsymbol{x}\in\partial\mathcal{O}, \qquad \boldsymbol{u}(s,\boldsymbol{x}) = \boldsymbol{\phi}(s,\boldsymbol{x}), \quad s\in[-r,0], \end{aligned} \tag{1}$$

where n denotes the number of neurons, $\boldsymbol{u} = (u_1, u_2, \dots, u_n)^{\mathrm{T}}$ is the state vector, which is a function with independent variable $t\in\mathbb{R}$, and space $\boldsymbol{x}\in\mathcal{O}$. $\mathcal{O}\subset\mathbb{R}^l$ is a connected bounded set with smooth boundary $\partial\mathcal{O}$. The general gradient operator of state vector $\boldsymbol{u}$ is defined as $\nabla\boldsymbol{u} = (\nabla u_1, \nabla u_2, \dots, \nabla u_n)^{\mathrm{T}}$, where $\nabla u_i = (\partial u_i/\partial x_1, \partial u_i/\partial x_2, \dots, \partial u_i/\partial x_l)^{\mathrm{T}}$, $i = 1, 2, \dots, n$, so the size of $\nabla\boldsymbol{u}$ is $n\times l$. $\boldsymbol{f}(\boldsymbol{u}) = (f_1(u_1), f_2(u_2), \dots, f_n(u_n))^{\mathrm{T}}$ is a diagonal map, which represents continuous activation function. $\boldsymbol{A} = \mathrm{diag}(a_1, a_2, \dots, a_n)$, $a_i > 0$, $i = 1, 2, \dots, n$, is the matrix of self-inhibition rate. $\boldsymbol{C} = (c_{ij})_{n\times n}$ represents matrix of connection weights between neurons. $\boldsymbol{I} = (I_1, I_2, \dots, I_n)^{\mathrm{T}}$ is the external bias vector, and $\boldsymbol{\phi}(s,\boldsymbol{x}) = (\phi_1(s,\boldsymbol{x}), \phi_2(s,\boldsymbol{x}), \dots, \phi_n(s,\boldsymbol{x}))^{\mathrm{T}} \in \mathfrak{L}^2_{\mathcal{F}_0}([-r,0];U)$ is the initial function. $D(x) = (D_{ij})_{n\times l}$ is the diffusion coefficient matrix, the value of which is determined by Fick's law [8]. Let $Y = (y_{ij})_{n\times l} = D\circ\nabla\boldsymbol{u} = (D_{ij}(\partial u_i/\partial x_j))_{n\times l}$ is the Hadamard product of matrix D and $\nabla\boldsymbol{u}$. $\nabla\cdot Y$ is the general divergence operator of matrix Y, which is defined as $\nabla\cdot Y = (\nabla\cdot\boldsymbol{Y}_1, \nabla\cdot\boldsymbol{Y}_2, \dots, \nabla\cdot\boldsymbol{Y}_n)^{\mathrm{T}}$, $\boldsymbol{Y}_i$, $i = 1, 2, \dots, n$, is the ith column of matrix Y. $\nabla\cdot\boldsymbol{Y}_i$ is the divergence operator of vector $\boldsymbol{Y}_i$. The boundary condition is $\partial\boldsymbol{u}/\partial\nu = (\partial u_1/\partial\nu, \partial u_2/\partial\nu, \dots, \partial u_n/\partial\nu)^{\mathrm{T}}$, $\partial u_i/\partial\nu = (\partial u_i/\partial x_1, \partial u_i/\partial x_2, \dots, \partial u_i/\partial x_m)^{\mathrm{T}}$, $i = 1, 2, \dots, n$. Adiabatic boundary condition is used in this article.

r is the length of time delay. In this article, the delay is expressed as a Lebesgue–Stieltjes integral, which is called s-delay. Specifically,

$$\int_{-r}^{0}\boldsymbol{u}(t+s,\,\boldsymbol{x})\,\mathrm{d}\eta(s) = \left(\int_{-r}^{0}u_1(t+s,\,\boldsymbol{x})\,\mathrm{d}\eta_1(s),\ \dots,\ \int_{-r}^{0}u_n(t+s,\,\boldsymbol{x})\,\mathrm{d}\eta_n(s)\right)^{\mathrm{T}}.$$

$\eta_i(s)$, $i = 1, 2, \dots, n$, are nondecreasing functions with bounded variation. In other words, there exist constants q_i, $i = 1, 2, \dots, n$, such that $\int_{-r}^{0}\mathrm{d}\eta_i(s) = q_i$. For convenience of study, we construct the matrix $\widetilde{Q} = \mathrm{diag}\{q_1, q_2, \dots, q_n\}$.

Let $\boldsymbol{u}_d$ denotes the state vector of drive system, which satisfies

$$\begin{aligned} \mathrm{d}\boldsymbol{u}_d &= \Bigg(\nabla\cdot\big(D(\boldsymbol{x})\circ\nabla\boldsymbol{u}_d\big) - \boldsymbol{A}\boldsymbol{u}_d + \boldsymbol{I} + P\boldsymbol{v} \\ &\qquad + \boldsymbol{C}\boldsymbol{f}\left(\int_{-r}^{0}\boldsymbol{u}_d(t+s,\,\boldsymbol{x})\,\mathrm{d}\eta(s)\right)\Bigg)\mathrm{d}t + \boldsymbol{g}(\boldsymbol{u}_d-\boldsymbol{u})\,\mathrm{d}\boldsymbol{W} \\ \frac{\partial\boldsymbol{u}_d}{\partial\nu}&(t,\boldsymbol{x}) = 0, \quad t\geqslant 0,\ \boldsymbol{x}\in\partial\mathcal{O}, \qquad \boldsymbol{u}_d(s,\boldsymbol{x}) = \boldsymbol{\psi}(s,\boldsymbol{x}), \quad s\in[-r,0], \end{aligned} \tag{2}$$

with $\boldsymbol{\psi(s,x)} = (\psi_1(s,\boldsymbol{x}), \psi_2(s,\boldsymbol{x}), \dots, \psi_n(s,\boldsymbol{x}))^{\mathrm{T}} \in \mathfrak{L}^2_{\mathcal{F}_0}([-r,0];U)$, $\boldsymbol{u}_d = (u_d^1, u_d^2, \dots, u_d^n)$. $\boldsymbol{g}(\boldsymbol{u}_d - \boldsymbol{u})$ is the intensity of noise, it is a matrix-valued function. $\boldsymbol{g}$ is inferred from the occurrence of eternal random fluctuation and other probabilistic causes. $\boldsymbol{u}$ is the solution of (1). $\boldsymbol{v} = (v_1, v_2, \dots, v_m)$ is the control input of this system. $P \in \mathbb{R}^{n\times m}$ is the gain of $\boldsymbol{v}$, which is a dimensionless control matrix and has full column rank. Other symbols have the same physical meaning as those in (1).

Remark 1. If

$$\eta_i(s) = \begin{cases} 0, & -r \leqslant s < 0 \\ 1, & s = 0,\ i = 1, 2, \dots, n. \end{cases}$$

Then by calculating the Lebesgue–Stieltjes integral, the governing equation of (1) is transformed to

$$\mathrm{d}\boldsymbol{u} = \big(\nabla \cdot \big(D(\boldsymbol{x}) \circ \nabla \boldsymbol{u}\big) - \boldsymbol{A}\boldsymbol{u} + \boldsymbol{C}\boldsymbol{f}\big(\boldsymbol{u}(t-r,\, \boldsymbol{x})\big) + \boldsymbol{I}\big)\,\mathrm{d}t,$$

which is the system with discrete delay as that in [8].

If there exists function $\boldsymbol{\kappa}(s)$ such that $\mathrm{d}\boldsymbol{\eta}(s) = \boldsymbol{\kappa}(s)\,\mathrm{d}s$, by calculating the Lebesgue–Stieltjes integral, the governing equation of response system is reduced to

$$\mathrm{d}\boldsymbol{u} = \left(\nabla \cdot \big(D(\boldsymbol{x}) \circ \nabla \boldsymbol{u}\big) - \boldsymbol{A}\boldsymbol{u} + \boldsymbol{C}\boldsymbol{f}\left(\int_{-r}^{0} \boldsymbol{u}(t+s,\, \boldsymbol{x})\kappa(s)\,\mathrm{d}s\right) + \boldsymbol{I}\right)\mathrm{d}t,$$

which is the system with distributed delays. That means that our model is more general than those studied before.

2.1 Tracking error in the Hilbert space

The tracking error vector $\boldsymbol{e}(t)$ is defined as the difference between the observed behavior of the drive system (2) and its desired behavior of response system (1):

$$\boldsymbol{e}(t,\boldsymbol{x}) = \boldsymbol{u}_d(t,\boldsymbol{x}) - \boldsymbol{u}(t,\boldsymbol{x}). \tag{3}$$

From (1)–(3) we get the following error dynamics:

$$\begin{aligned}
\mathrm{d}\boldsymbol{e} &= \left(P\boldsymbol{v} + \nabla \cdot \big(D(\boldsymbol{x}) \circ \nabla \boldsymbol{e}\big) - \boldsymbol{A}\boldsymbol{e} + \boldsymbol{C}\boldsymbol{f}\left(\int_{-r}^{0} \boldsymbol{u}_d(t+s,\, \boldsymbol{x})\,\mathrm{d}\eta(s)\right)\right. \\
&\quad \left. - \boldsymbol{C}\boldsymbol{f}\left(\int_{-r}^{0} \boldsymbol{u}(t+s,\, \boldsymbol{x})\,\mathrm{d}\eta(s)\right)\right)\mathrm{d}t + \boldsymbol{g}(\boldsymbol{e})\,\mathrm{d}\boldsymbol{W}, \\
&\frac{\partial \boldsymbol{e}}{\partial \nu}(t,\boldsymbol{x}) = 0, \quad t \geqslant 0,\ \boldsymbol{x} \in \partial\mathcal{O}, \\
&\boldsymbol{e}(s,x) = -\boldsymbol{\phi}(s,\boldsymbol{x}) + \boldsymbol{\psi}(s,\boldsymbol{x}), \quad \boldsymbol{x} \in \mathcal{O},\ s \in [-r,0].
\end{aligned} \tag{4}$$

Let us define the diffusion operator as follows:

$$\mathfrak{A} : \mathcal{D}(\mathfrak{A}) \to U, \quad \mathfrak{A}\boldsymbol{e} = \nabla \cdot \big(D(\boldsymbol{x}) \circ \nabla \boldsymbol{e}\big),$$

where $\mathcal{D}(\mathfrak{A})$ is the domain of $\mathfrak{A}$ defined as $\mathcal{D}(\mathfrak{A}) = \{\boldsymbol{e}\colon \boldsymbol{e} \in \{H^2(\mathcal{O})\}^n,\ \partial\boldsymbol{e}/\partial\nu|_{\partial\mathcal{O}} = \boldsymbol{0}\}$.

We rewrite system (4) in the following form of stochastic functional differential equations in Hilbert space:

$$\begin{aligned} &\mathrm{d}\boldsymbol{e} = (P\boldsymbol{v} + \mathfrak{A}\boldsymbol{e} - \boldsymbol{A}\boldsymbol{e} + \boldsymbol{C}\widetilde{\boldsymbol{f}})\,\mathrm{d}t + \boldsymbol{g}(\boldsymbol{e})\,\mathrm{d}\boldsymbol{W} \\ &\boldsymbol{e}(s) = \boldsymbol{\psi}(s) - \boldsymbol{\phi}(s), \quad s \in [-r, 0], \end{aligned} \tag{5}$$

where $\widetilde{\boldsymbol{f}} = \boldsymbol{f}(\int_{-r}^{0} \boldsymbol{u}_d(t+s)\,\mathrm{d}\eta) - \boldsymbol{f}(\int_{-r}^{0} \boldsymbol{u}(t+s)\,\mathrm{d}\eta)$, $(\boldsymbol{\psi} - \boldsymbol{\phi}) \in \mathfrak{L}^2_{\mathcal{F}_0}([-r,0]; U)$.

The basic assumptions are

- (H1) $|f_i(u_i) - f_i(v_i)| \leqslant \sigma_i |u_i - v_i|$ for all $u_i, v_i \in \mathbb{R}$, $\sigma_i > 0$, $i = 1, 2, \dots, n$;
- (H2) There exist two positive constants α, β such that $0 < \alpha \leqslant D_{ij} \leqslant \beta$;
- (H3) The noise intensifying function $\boldsymbol{g}(\boldsymbol{u})$ satisfies the linear growth constraints, which means that there exists a positive constant k such that $\operatorname{tr}(\boldsymbol{g}^{\mathrm{T}}\boldsymbol{g}) \leqslant k(\boldsymbol{u}^{\mathrm{T}}\boldsymbol{u})$;
- (H4) $\gamma - \gamma^{-1} n \|KC\|_F^2 \|\Sigma\tilde{Q}\|_F^2 > 0$, $a_m = \min\{a_1, a_2, \dots, a_n\}$, $\gamma = \zeta_m a_m - \lambda_M(K)k > 0$, $\zeta_m = \lambda_m(K)$, K will be defined in (8), and $\tilde{K}$ is a semipositive definite matrix.

Remark 2. From [8] we know that global Lipschitz condition (H1) and positiveness of diffusion coefficients (H2) can ensure the existence and uniqueness of (1). Moreover, the noise intensifying function depends on the state vector of the error system, and it is a nonlinear function rather than a linear function. (H3) means that the noise intensity is upper bounded by the norm of error. The noise is removed if the error vanishes. Furthermore, the surface will become smoother if $\boldsymbol{e} \to \boldsymbol{0}$. Last, from (H1) the requirement of monotonicity, continuously differentiable restriction, and boundedness of activation function is removed. So this type of activation function is more general than the sigmoid activation functions studied in [11, 23, 30].

We can infer from (H1) that

Lemma 1. *If $\boldsymbol{f}$ is a diagonal map and satisfies* (H1)*, we can get*

$$\|\tilde{\boldsymbol{f}}\|^2 \leqslant \|\Sigma\widetilde{Q}\|_F^2 \|\boldsymbol{e}_t\|_C^2,$$

where $\Sigma = \operatorname{diag}\{\sigma_1, \sigma_2, \dots, \sigma_n\}$.

By using (H1) and total boundedness of Lebesgue–Stieltjes integral $\int_{-r}^{0} \mathrm{d}\eta(s)$, we have

$$\begin{aligned} &\int_{\mathcal{O}} \left| f_i\left(\int_{-r}^{0} u_d^i(t+s,\, \boldsymbol{x})\,\mathrm{d}\eta_i(s)\right) - f_i\left(\int_{-r}^{0} u_i(t+s,\, \boldsymbol{x})\,\mathrm{d}\eta_i(s)\right)\right|^2 \mathrm{d}\boldsymbol{x} \\ &\quad \leqslant \sigma_i^2 \int_{\mathcal{O}} \left|\int_{-r}^{0} e_i(t+s,\, \boldsymbol{x})\,\mathrm{d}\eta_i(s)\right|^2 \mathrm{d}\boldsymbol{x} \leqslant \sigma_i^2 q_i^2 \int_{\mathcal{O}} \sup_{s\in[-r,0]} e_i^2(t+s,\, \boldsymbol{x})\,\mathrm{d}\boldsymbol{x} \\ &\quad = \sigma_i^2 q_i^2 \sup_{s\in[-r,0]} \big\|e_i(t+s)\big\|^2_{L^2(\mathcal{O})}. \end{aligned}$$

By the definition of $\tilde{\boldsymbol{f}}$, $\|\cdot\|_F$, $\|\boldsymbol{e}_t\|_C$, as well as $\boldsymbol{f}$ is a diagonal map, one obtains

$$\|\tilde{\boldsymbol{f}}\|^2 \leqslant \|\Sigma\widetilde{Q}\|_F^2 \sup_{s\in[-r,0]} \big\|\boldsymbol{e}(t+s)\big\|^2 = \|\Sigma\widetilde{Q}\|_F^2 \|\boldsymbol{e}_t\|_C^2.$$

Let us construct a new matrix $\widetilde{K} = (\widetilde{k}_{ij})_{n\times n}$ based on $K = (k_{ij})_{n\times n}$ with $\widetilde{k}_{ii} = k_{ii}\alpha$ and $\widetilde{k}_{ij} = -|k_{ij}|\beta$, $i \neq j$. Then we have

Lemma 2. *If* (H2) *holds and* $\widetilde{K}$ *is a semipositive definite matrix, then we have* $(\boldsymbol{u}, K\mathfrak{A}\boldsymbol{u}) \leqslant 0$, $\boldsymbol{u} \in U$.

By using the property of Hadmard product and the basic relationship between divergence operator and gradient operator, we first prove the following equality, which is expressed as

$$\nabla \cdot (u_i \boldsymbol{Y}_i) = u_i \nabla \cdot (\boldsymbol{Y}_i) + \langle \nabla u_i,\, \boldsymbol{Y}_i\rangle,$$

where $\langle\cdot,\cdot\rangle$ denotes the standard inner product of Euclid space $\mathbb{R}^l$. Then we have

$$\begin{aligned}
&\nabla \cdot \big(\operatorname{diag}(u_1, u_2, \dots, u_n) K Y\big) \\
&\quad = \nabla \cdot \big(\operatorname{diag}(u_1, u_2, \dots, u_n) K (\boldsymbol{Y}_1, \dots, \boldsymbol{Y}_n)^{\mathrm{T}}\big) \\
&\quad = \nabla \cdot \left(\begin{pmatrix} k_{11}u_1 & \dots & k_{1n}u_n \\ k_{21}u_1 & \dots & k_{2n}u_n \\ \dots & \dots & \dots \\ k_{n1}u_1 & \dots & k_{nn}u_n \end{pmatrix} (\boldsymbol{Y}_1, \dots, \boldsymbol{Y}_n)^{\mathrm{T}} \right) \\
&\quad = \nabla \cdot \left(\sum_{j=1}^n k_{1j} u_j \boldsymbol{Y}_j,\ \sum_{j=1}^n k_{2j} u_j \boldsymbol{Y}_j,\ \dots,\ \sum_{j=1}^n k_{nj} u_j \boldsymbol{Y}_j \right)^{\mathrm{T}} \\
&\quad = \left(\sum_{j=1}^n k_{1j} u_j \nabla\cdot \boldsymbol{Y}_j + \sum_{j=1}^n k_{1j} \langle \nabla u_j, \boldsymbol{Y}_j\rangle, \right. \\
&\qquad \sum_{j=1}^n k_{2j} u_j \nabla\cdot \boldsymbol{Y}_j + \sum_{j=1}^n k_{2j} \langle \nabla u_j, \boldsymbol{Y}_j\rangle,\ \dots, \\
&\qquad \left. \sum_{j=1}^n k_{nj} u_j \nabla\cdot \boldsymbol{Y}_j + \sum_{j=1}^n k_{nj} \langle \nabla u_j, \boldsymbol{Y}_j\rangle \right)^{\mathrm{T}} \\
&\quad = \operatorname{diag}(u_1, u_2, \dots, u_n) K \nabla Y \\
&\qquad + \begin{pmatrix} k_{11} & k_{12} & \dots & k_{1n} \\ k_{21} & k_{22} & \dots & k_{2n} \\ \dots & \dots & \dots & \dots \\ k_{n1} & k_{n2} & \dots & k_{nn} \end{pmatrix} \begin{pmatrix} \langle \nabla u_1, Y_1\rangle \\ \langle \nabla u_2, Y_2\rangle \\ \dots \\ \langle \nabla u_n, Y_n\rangle \end{pmatrix}
\end{aligned}$$

with $Y = (\boldsymbol{Y}_1, \dots, \boldsymbol{Y}_n)^{\mathrm{T}}$.

On the other side, by using the definition of Hadmard product, we have

$$\begin{pmatrix} \langle \nabla u_1, Y_1 \rangle \\ \langle \nabla u_2, Y_2 \rangle \\ \cdots \\ \langle \nabla u_n, Y_n \rangle \end{pmatrix} = \begin{pmatrix} \frac{\partial u_1}{\partial x_1} y_{11} + \frac{\partial u_1}{\partial x_2} y_{12} + \cdots + \frac{\partial u_1}{\partial x_l} y_{1l} \\ \frac{\partial u_2}{\partial x_1} y_{21} + \frac{\partial u_2}{\partial x_2} y_{22} + \cdots + \frac{\partial u_2}{\partial x_l} y_{2l} \\ \cdots \\ \frac{\partial u_2}{\partial x_1} y_{n1} + \frac{\partial u_2}{\partial x_2} y_{n2} + \cdots + \frac{\partial u_n}{\partial x_l} y_{nl} \end{pmatrix}$$

$$= \left(\begin{pmatrix} \frac{\partial u_1}{\partial x_1} & \cdots & \frac{\partial u_1}{\partial x_l} \\ \frac{\partial u_2}{\partial x_1} & \cdots & \frac{\partial u_2}{\partial x_l} \\ \cdots & \cdots & \cdots \\ \frac{\partial u_n}{\partial x_1} & \cdots & \frac{\partial u_n}{\partial x_l} \end{pmatrix} \circ \begin{pmatrix} y_{11} & \cdots & y_{1l} \\ y_{21} & \cdots & y_{2l} \\ \cdots & \cdots & \cdots \\ y_{n1} & \cdots & y_{nl} \end{pmatrix} \right) \boldsymbol{J}, \tag{6}$$

where $\boldsymbol{J} = (1, 1, \ldots, 1)^{\mathrm{T}}$, which means that

$$\nabla \cdot \big(\mathrm{diag}(u_1, u_2, \ldots, u_n) K Y\big) = \mathrm{diag}(u_1, u_2, \ldots, u_n) K \nabla Y + K\big((\nabla \boldsymbol{u} \circ Y)\boldsymbol{J}\big).$$

In other words, we have

$$\mathrm{diag}(u_1, u_2, \ldots, u_n) K \nabla Y = \nabla \cdot \big(\mathrm{diag}(u_1, u_2, \ldots, u_n) K Y\big) - K\big((\nabla \boldsymbol{u} \circ Y)\boldsymbol{J}\big).$$

Let $Y = D(\boldsymbol{x}) \circ \nabla u$ in (6), and using the general Gauss formula for the matrix

$$\begin{aligned} \int_{\mathcal{O}} \nabla \cdot Z \, \mathrm{d}\boldsymbol{x} &= \int_{\mathcal{O}} \nabla \cdot (\boldsymbol{Z}_1, \boldsymbol{Z}_2, \ldots, \boldsymbol{Z}_n)^{\mathrm{T}} \, \mathrm{d}\boldsymbol{x} \\ &= \bigg(\int_{\mathcal{O}} \nabla \cdot \boldsymbol{Z}_1 \, \mathrm{d}\boldsymbol{x}, \ \int_{\mathcal{O}} \nabla \cdot \boldsymbol{Z}_2 \, \mathrm{d}\boldsymbol{x}, \ \ldots, \ \int_{\mathcal{O}} \nabla \cdot \boldsymbol{Z}_n \, \mathrm{d}\boldsymbol{x} \bigg)^{\mathrm{T}} \\ &= \bigg(\int_{\partial\mathcal{O}} \boldsymbol{Z}_1 \, \mathrm{d}s, \ \int_{\partial\mathcal{O}} \nabla \cdot \boldsymbol{Z}_2 \, \mathrm{d}s, \ \ldots, \ \int_{\partial\mathcal{O}} \boldsymbol{Z}_n \, \mathrm{d}s \bigg)^{\mathrm{T}} \\ &= \int_{\partial\mathcal{O}} \nabla \cdot (\boldsymbol{Z}_1, \boldsymbol{Z}_2, \ldots, \boldsymbol{Z}_n)^{\mathrm{T}} \, \mathrm{d}s = \int_{\partial\mathcal{O}} Z \, \mathrm{d}s, \end{aligned}$$

where $\boldsymbol{Z}_i$ is the ith column of Z, and the adiabatic boundary conditions, we have

$$\begin{aligned} &\int_{\mathcal{O}} \mathrm{diag}(u_1, u_2, \ldots, u_n) K \nabla \cdot \big(D(\boldsymbol{x}) \circ \nabla \boldsymbol{u}\big) \, \mathrm{d}\boldsymbol{x} \\ &\quad = \int_{\mathcal{O}} \nabla \cdot \big(\mathrm{diag}(u_1, \ldots, u_n) K (D(\boldsymbol{x}) \circ \nabla \boldsymbol{u})\big) \, \mathrm{d}\boldsymbol{x} \\ &\qquad - \int_{\mathcal{O}} K\big(\big(\nabla \boldsymbol{u} \circ \big(D(\boldsymbol{x}) \circ \nabla \boldsymbol{u}\big)\big)\boldsymbol{J}\big) \, \mathrm{d}\boldsymbol{x} \\ &\quad = \int_{\partial\mathcal{O}} \mathrm{diag}(u_1, u_2, \ldots, u_n) K \big(D(\boldsymbol{x}) \circ \nabla \boldsymbol{u}\big) \, \mathrm{d}\boldsymbol{x} \end{aligned}$$

$$
\begin{aligned}
&- \int\limits_{\mathcal{O}} K\big(\big(\nabla \boldsymbol{u} \circ \big(D(\boldsymbol{x}) \circ \nabla \boldsymbol{u}\big)\big)\boldsymbol{J}\big)\,\mathrm{d}\boldsymbol{x} \\
&= - \int\limits_{\mathcal{O}} K\big(\big(\nabla \boldsymbol{u} \circ \big(D(\boldsymbol{x}) \circ \nabla \boldsymbol{u}\big)\big)\boldsymbol{J}\big)\,\mathrm{d}\boldsymbol{x}.
\end{aligned}
$$

For the relationship between inner product, Hadmard product, and Kronecker product, we have

$$
\prec \boldsymbol{u}, \boldsymbol{v} \succ = \operatorname{tr}\big(\boldsymbol{u} \otimes \boldsymbol{v}^{\mathrm{T}}\big) = \operatorname{sum}(\boldsymbol{u} \circ \boldsymbol{v}), \quad \boldsymbol{u}, \boldsymbol{v} \in \mathbb{R}^n, \tag{7}
$$

where $\prec \boldsymbol{u}, \boldsymbol{v} \succ$ denotes the inner product of $\mathbb{R}^n$, $\otimes$ denotes the Kronecker product of two matrix. $\operatorname{sum}(\boldsymbol{u}) = \sum_{i=1}^n u_i$, $\boldsymbol{u} = (u_1, u_2, \dots, u_n)^{\mathrm{T}}$.

Then by using (H2), (7), Cauchy inequality $(\boldsymbol{u}, \boldsymbol{v}) \leqslant \|\boldsymbol{u}\|\|\boldsymbol{v}\|$, and $(\boldsymbol{u}, \boldsymbol{u}) = \|\boldsymbol{u}\|^2$, we have

$$
\begin{aligned}
(\boldsymbol{e}, K\mathfrak{A}\boldsymbol{e}) &= - \int\limits_{\mathcal{O}} \sum_{i=1}^n \sum_{j=1}^n k_{ij} \langle \nabla u_i,\, D_j \circ \nabla u_j \rangle \,\mathrm{d}\boldsymbol{x} \\
&\leqslant - \int\limits_{\mathcal{O}} \sum_{i=1}^n k_{ii} \langle \nabla u_i,\, D_i \circ \nabla u_i \rangle \mathrm{d}\boldsymbol{x} - \int\limits_{\mathcal{O}} \sum_{i \neq j} k_{ij} \langle \nabla u_i,\, D_j \circ \nabla u_j \rangle \,\mathrm{d}\boldsymbol{x} \\
&\leqslant -\boldsymbol{u}_+ \widetilde{K} \boldsymbol{u}_+^{\mathrm{T}},
\end{aligned}
$$

where $\boldsymbol{u}_+ = (\|\nabla u_1\|,\, |\nabla u_2\|,\, \dots,\, \|\nabla u_n\|)$. Since $\widetilde{K}$ is a positive definite matrix, then we have

$$
(\boldsymbol{e}, K\mathfrak{A}\boldsymbol{e}) \leqslant 0.
$$

Lemma 3 [Hanalay inequality]. *If $u \geqslant 0$ and meets*

$$
\begin{aligned}
&\frac{\mathrm{d}u}{\mathrm{d}t} \leqslant -au + b \sup_{-r \leqslant \theta \leqslant 0} u(t+\theta), \\
&u(\theta) = \phi(\theta), \quad \phi \in C\big([-r, 0], \mathbb{R}\big),
\end{aligned}
$$

where $a, b > 0$, $a - b > 0$, then there are positive scalars k and D such that

$$
u \leqslant k \exp\{-Dt\}.
$$

3 Switching surface and design of controller

In this work, the switching surface is constructed as a linear function of the current states

$$
s_0 = \big\{\boldsymbol{e} \in U\colon\ \boldsymbol{S}(\boldsymbol{e}) = P^{\mathrm{T}} K \boldsymbol{e} = \boldsymbol{0}\big\}, \tag{8}
$$

$K \in \mathbb{R}^{n \times n}$ will be determined later, and we assume that it meets the condition $K > 0$.

The switching control law is defined as

$$\boldsymbol{v}(\boldsymbol{x},t) = -\tilde{B}(\mathfrak{A}\boldsymbol{e} - A\boldsymbol{e} + C\widetilde{\boldsymbol{f}}) - (P^{\mathrm{T}}KP)^{-1}\left(\varrho\boldsymbol{S} + \varepsilon\frac{\boldsymbol{S}}{\|\boldsymbol{S}\|}\right), \tag{9}$$

where $\tilde{B} = (P^{\mathrm{T}}KP)^{-1}P^{\mathrm{T}}K$. ε and ϱ are positive scalars, which will be selected properly.

Remark 3. The discontinuous term $\boldsymbol{S}/\|\boldsymbol{S}\|$ in (9) can be replaced with the continuous term $\boldsymbol{S}/(\|\boldsymbol{S}\| + \tau)$, where $\tau > 0$ is a small number. It is determined through experience. Then control law (9) is replaced with

$$\boldsymbol{v}(\boldsymbol{x},t) = -\tilde{B}(\mathfrak{A}\boldsymbol{e} - A\boldsymbol{e} + C\widetilde{\boldsymbol{f}}) - \left(P^{\mathrm{T}}KP\right)^{-1}\left(\varrho\boldsymbol{S} + \varepsilon\frac{\boldsymbol{S}}{\|\boldsymbol{S}\| + \tau}\right).$$

This treatment can be used to eliminate chattering. However, the robustness of the system will also be removed if this continuation controller is used.

4 Synchronization of SRDHNNs with s-delays under SMC

We have the following main theorem of this article.

Theorem 1. *Let system* (5) *satisfy* (H1)–(H4). *Suppose that the switching surface is given by* (8)*, and the SMC law is set to be* (9). *Then the solution of* (5) *is exponentially stable in the mean-square sense on the switching surface described by* (8). *In other words,* (1) *and* (2) *is exponentially synchronized in the mean-square sense under* (9) *on the switching surface described by* (8).

Proof. Let us define the Lyapunov–Krasovskii functional as follows:

$$V\big((\boldsymbol{e})_t\big) = \big\|(\boldsymbol{e})_{\boldsymbol{t}}(0)\big\|_K^2 \triangleq \int\limits_{\mathcal{O}} \boldsymbol{e}^{\mathrm{T}}(t)K\boldsymbol{e}(t)\,\mathrm{d}\boldsymbol{x}, \tag{10}$$

$K > 0$ is the same matrix as that in (8).

By Itô's formula, we have

$$\mathrm{d}V = \mathcal{L}V\,\mathrm{d}t + 2\int\limits_{\mathcal{O}} \boldsymbol{e}^{\mathrm{T}}K\boldsymbol{g}\,\mathrm{d}\boldsymbol{W}\,\mathrm{d}\boldsymbol{x}, \tag{11}$$

where

$$\begin{aligned}\mathcal{L}V = {}& 2\int\limits_{\mathcal{O}} \boldsymbol{e}^{\mathrm{T}}K\mathfrak{A}\boldsymbol{e}\,\mathrm{d}\boldsymbol{x} + 2\int\limits_{\mathcal{O}} \boldsymbol{e}^{\mathrm{T}}KA\boldsymbol{e}\,\mathrm{d}\boldsymbol{x} + 2\int\limits_{\mathcal{O}} \boldsymbol{e}^{\mathrm{T}}KC\widetilde{\boldsymbol{f}}\,\mathrm{d}\boldsymbol{x} \\ &+ 2\int\limits_{\mathcal{O}} \boldsymbol{e}^{\mathrm{T}}KP\boldsymbol{v}\,\mathrm{d}\boldsymbol{x} + \int\limits_{\mathcal{O}} \mathrm{tr}\big(\boldsymbol{g}^{\mathrm{T}}K\boldsymbol{g}\big)\,\mathrm{d}\boldsymbol{x}\end{aligned}$$

$$
\begin{aligned}
&= 2\int\limits_{\mathcal{O}} \boldsymbol{e}^{\mathrm{T}} K \mathfrak{A} \boldsymbol{e}\,\mathrm{d}\boldsymbol{x} + 2\int\limits_{\mathcal{O}} \boldsymbol{e}^{\mathrm{T}} K A \boldsymbol{e}\,\mathrm{d}\boldsymbol{x} \\
&\quad + 2\int\limits_{\mathcal{O}} \boldsymbol{e}^{\mathrm{T}} K C \widetilde{\boldsymbol{f}}\,\mathrm{d}\boldsymbol{x} + \int\limits_{\mathcal{O}} \operatorname{tr}\bigl(\boldsymbol{g}^{\mathrm{T}} K \boldsymbol{g}\bigr)\,\mathrm{d}\boldsymbol{x}.
\end{aligned} \tag{12}
$$

By Lemma 2 and the semipositiveness of the matrix $\widetilde{K}$, we get

$$
\int\limits_{\mathcal{O}} \boldsymbol{e}^{\mathrm{T}} K \mathfrak{A} \boldsymbol{e}\,\mathrm{d}\boldsymbol{x} \leqslant 0. \tag{13}
$$

By the positiveness of diagonal entries of A (so KA is a positive definite matrix), we have

$$
-\int\limits_{\mathcal{O}} \boldsymbol{e}^{\mathrm{T}} K A \boldsymbol{e}\,\mathrm{d}\boldsymbol{x} \leqslant -\zeta_m a_m \|\boldsymbol{e}\|^2. \tag{14}
$$

By (H3), we obtain

$$
\int\limits_{\mathcal{O}} \operatorname{tr}\bigl(\boldsymbol{g}^{\mathrm{T}} K \boldsymbol{g}\bigr)\,\mathrm{d}\boldsymbol{x} \leqslant \lambda_M(K) \int\limits_{\mathcal{O}} \operatorname{tr}\bigl(\boldsymbol{g}^{\mathrm{T}} \boldsymbol{g}\bigr)\,\mathrm{d}\boldsymbol{x} \leqslant \lambda_M(K) k \|\mathbf{e}\|^2. \tag{15}
$$

By Young inequality, Lemma 1, the definition of $\tilde{\boldsymbol{f}}$ ($\boldsymbol{f}$ is a diagonal map), condition (H1), and total variation boundedness of Lebesgue–Stieltjes integral $\int_{-r}^{0} \mathrm{d}\eta_i(s) = q_i > 0$, $i = 1, 2, \dots, n$, we have

$$
\begin{aligned}
\bigl(\boldsymbol{e(t)}, KC\widetilde{\boldsymbol{f}}\bigr) &\leqslant \frac{\gamma}{2}\|\boldsymbol{e}\|^2 + \frac{1}{2}\gamma^{-1}\|KC\widetilde{\boldsymbol{f}}\|^2 \\
&\leqslant \frac{\gamma}{2}\|\boldsymbol{e}\|^2 + \frac{n}{2}\gamma^{-1}\|KC\|_F^2\|\widetilde{\boldsymbol{f}}\|^2 \\
&\leqslant \frac{1}{2}\gamma\|\boldsymbol{e}\|^2 + \frac{n}{2}\gamma^{-1}\|KC\|_F^2\|\Sigma\tilde{Q}\|_F^2\|\boldsymbol{e}_t\|_C^2.
\end{aligned} \tag{16}
$$

By (10)–(16), we have

$$
\mathcal{L}V \leqslant -\gamma V + c_1 \sup_{s\in[-r,0]} V(t+s)
$$

with $c_1 = \gamma^{-1}\|KC\|_F^2\|\Sigma\tilde{Q}\|_F^2$. By Itô's formula, we have

$$
\mathsf{E}V \leqslant -\gamma \mathsf{E}V + c_1 \sup_{s\in[-r,0]} \mathsf{E}V(t+s).
$$

From (H4) we have $\gamma > c_1$. By the Hanalay inequality, we have $\mathsf{E}V(t) \leqslant \mathsf{E}\|\boldsymbol{\phi} - \boldsymbol{\psi}\|_C \times \exp\{-(\gamma - c_1)t\}$. By definition of $\|\boldsymbol{e}_t\|_C$ in Section 2, (1) and (2) are exponentially synchronized in the mean-square sense under (9). □

5 Example and simulation

The response system is

$$\begin{aligned}
\mathrm{d}u_1 &= \left(\nabla\cdot\big(D_1(x)\nabla u_1\big) - 4u_1 + 0.5\tanh\left(\int_{-r}^{0} u_1(t+s,\,x)\,\mathrm{d}\eta\right)\right.\\
&\qquad \left. - 0.2\tanh\left(\int_{-r}^{0} u_2(t+s,\,x)\,\mathrm{d}\eta(s)\right) + I_1\right)\mathrm{d}t,\\
\mathrm{d}u_2 &= \left(\nabla\cdot\big(D_2(x)\nabla u_2\big) - 4u_2 - 5\tanh\left(\int_{-r}^{0} u_1(t+s,\,x)\,\mathrm{d}\eta\right)\right.\\
&\qquad \left. + 0.5\tanh\left(\int_{-r}^{0} u_2(t+s,\,x)\,\mathrm{d}\eta(ls)\right) + I_2\right)\mathrm{d}t,\\
&\frac{\partial u_i}{\partial x}(t,0) = \frac{\partial u_i}{\partial x}(t,20) = 0, \quad t \geqslant 0,\\
&u_1(s,x) = 3\cos(0.2\pi x), \qquad u_2(s,x) = -2\cos(0.2\pi x),\\
&x \in \mathcal{O} = [0,20], \quad s \in [-1,0], \quad i = 1,2,
\end{aligned} \tag{17}$$

and the drive system is

$$\begin{aligned}
\mathrm{d}u_d^1 &= \left(\nabla\cdot\big(D_1(x)\nabla u_d^1\big) - 4u_d^1 + 0.5\tanh\left(\int_{-r}^{0} u_d^1(t+s,\,x)\mathrm{d}\eta\right)\right.\\
&\qquad \left. - 0.2\tanh\left(\int_{-r}^{0} u_d^2(t+s,\,x)\,\mathrm{d}\eta(s)\right) + I_1 + p_1 v\right)\mathrm{d}t + e_1\,\mathrm{d}W,\\
\mathrm{d}u_d^2 &= \nabla\cdot\big(D_2(x)\nabla u_d^2\big) - 4u_d^2 - 5\tanh\left(\int_{-r}^{0} u_d^1(t+s,\,x)\,\mathrm{d}\eta\right.\\
&\qquad \left. + 0.5\tanh\left(\int_{-r}^{0} u_d^2(t+s,\,x)\,\mathrm{d}\eta(s)\right) + I_2 + p_2 v\right)\mathrm{d}t + e_2\,\mathrm{d}W,\\
&\frac{\partial u_d^i}{\partial x}(t,0) = \frac{\partial u_d^i}{\partial x}(t,20) = 0, \quad t \geqslant 0,\\
&u_d^1(s,x) = \cos(0.2\pi x), \qquad u_d^2(s,x) = -\cos(0.2\pi x),\\
&x \in \mathcal{O} = [0,20], \quad s \in [-1,0], \quad i = 1,2.
\end{aligned} \tag{18}$$

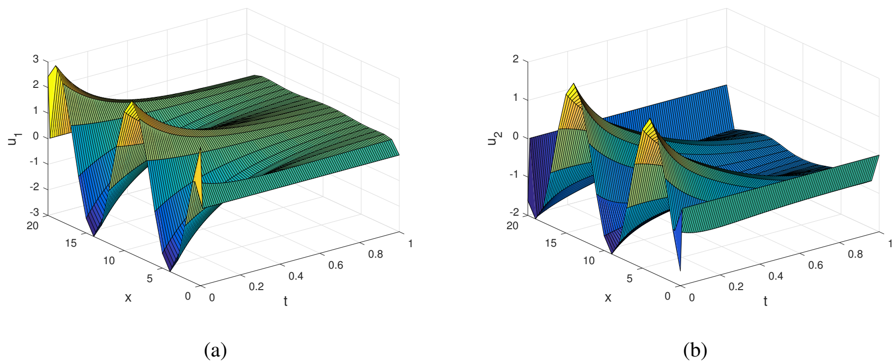

Figure 1. Simulation of u_1 and u_2 in response system (17).

In this example, $U = \{L^2(\mathcal{O})\}^2$, $\boldsymbol{u} = (u_1, u_2)^{\mathrm{T}} \in U$, $\boldsymbol{u}_d = (u_d^1, u_d^2)^{\mathrm{T}} \in U$,

$$\boldsymbol{\phi} = \bigl(3\cos(0.2\pi x), -2\cos(0.2\pi x)\bigr)^{\mathrm{T}} \in \mathfrak{L}^2_{\mathcal{F}_0}\bigl([-r, 0]; U\bigr),$$
$$\boldsymbol{\psi} = \bigl(\cos(0.2\pi x), \cos(0.2\pi x)\bigr)^{\mathrm{T}} \in \mathfrak{L}^2_{\mathcal{F}_0}\bigl([-r, 0]; U\bigr),$$

and

$$\boldsymbol{\phi} - \boldsymbol{\psi} = \bigl(2\cos(0.2\pi x), -3\cos(0.2\pi x)\bigr)^{\mathrm{T}} \in \mathfrak{L}^2_{\mathcal{F}_0}\bigl([-r, 0]; U\bigr),$$

W is one-dimensional standard Wiener process with mean zero. We can also see that $n=2$, $m=1$, $l=1$, $h=1$. In this example, time delay $r=1$ and s-type delay is defined as

$$\eta(s) = \begin{cases} 0, & -1 \leqslant s < 0, \\ 1, & s = 0. \end{cases}$$

Through calculating above Lebesgue–Stieljes integral, we get $\int_{-1}^{0} u_i(t+s, x)\,\mathrm{d}\eta(s) = u_i(t-1, x)$, $i = 1, 2$. This is also true for u_d^i. We also have $|\int_{-1}^{0} \mathrm{d}\eta(s)| \leqslant 1$ by calculation, so $q_1 = q_2 = 1$ is chosen, we also have $\widetilde{Q} = \operatorname{diag}\{q_1, q_2\}$. $\boldsymbol{f}$ is a diagonal map with $\boldsymbol{f} = (\tanh(u_1), \tanh(u_2))^{\mathrm{T}}$. By using $|\tanh(x) - \tanh(y)| < |x - y|$, $x, y \in \mathbb{R}$, so $f_1(u_1)$, $f_2(u_2)$ are global Lipschitz continuous functions with $\sigma_1 = 1$, $\sigma_2 = 1$ and $\sigma_M = 1$. This means that (H1) is satisfied in this system. Other parameters are as follows: $A = \left[\begin{smallmatrix} 4 & 0 \\ 0 & 4 \end{smallmatrix}\right]$ that means $\lambda_m(A) = \lambda_M(A) = 4$, $C = \left[\begin{smallmatrix} 0.5 & -0.2 \\ -5 & 0.5 \end{smallmatrix}\right]$, $I_1 = \left(\begin{smallmatrix} 5 \\ 2 \end{smallmatrix}\right)$, $P = \left(\begin{smallmatrix} 0.1 \\ 0.2 \end{smallmatrix}\right)$. By calculation, $\operatorname{rank}(P) = 1$, so it has full column rank. $D_1(x) = 1$, $D_2(x) = 1$ such that $\nabla \cdot (D_1(x)\nabla u_1) = \Delta u_1$, $\nabla \cdot (D_2(x)\nabla u_2) = \Delta u_2$, Δ is a Laplacian operator. By the way $0 < 1 \leqslant D_1(x) \leqslant 1$, $0 < 1 \leqslant D_2(x) \leqslant 1$, $\alpha = \beta = 1$, so (H2) is also fulfilled. Furthermore, $\boldsymbol{g} = (g_1, g_2)^{\mathrm{T}} = (e_1, e_2)^{\mathrm{T}}$, where $e_1 = u_d^1 - u_1$, $e_2 = u_d^2 - u_2$. By calculation, we get $k = 1$ in hypothesis (H3).

Matlab is used to perform the simulation. The code is written by ourselves and based on the finite difference method with space scale $\varDelta x = 1$ and time scale $\varDelta t = 0.01$. The second-order centered difference scheme is utilized to discrete the reaction–diffusion term. The Runge–Kutta–Chebyshev method is used to discrete the time. Euler–Maruyama formula is used to solve Wiener process. Relations $\mathsf{E}\varDelta W = 0$ and $\mathsf{E}(\varDelta W)^2 = \varDelta t$

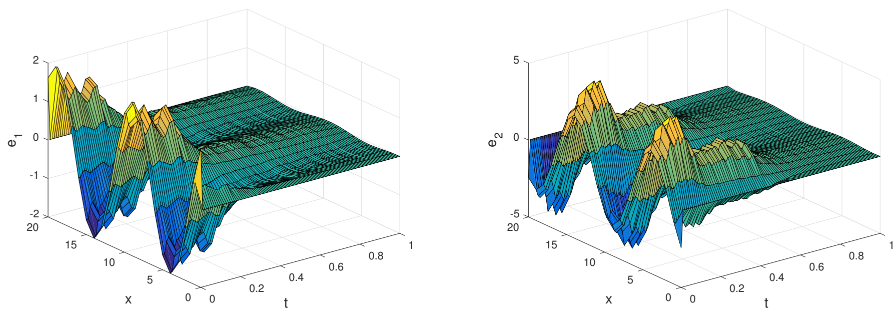

(a) (b)

Figure 2. Dynamical behavior of e_1 and e_2 without control in error system.

are also used for computing the Wiener increment. We first use this scheme to simulate the long time asymptotic behavior of response system (17). From Figs. 1(a), 1(b) the surface of reference system (17) is very complicated, especially, it seems that there is no equilibrium for $\boldsymbol{u}$. It will be a challenge to track this system. For the error system without control, it can be inferred from Figs. 2(a), 2(b) that solution even exhibits random oscillation in the whole process when driven by the Wiener process. To give a clear description of it, we also simulate the frequency of $\boldsymbol{e}$ in Fig. 3, which coincides with Figs. 2(a), 2(b). Now we devote ourselves to eliminate the noise and synchronize (17) and (18) under SMC.

In order to track the reference system (17), SMC law (9) is used to synchronize these two systems. So there are two main steps in the design of SMC. First, we design a switching surface, then we determine the control law based on the sliding mode. Appropriate switching surface and SMC law are based on Theorem 1. In the design of switching surface, we set $K = \operatorname{diag}(1,1)$, so $\lambda_m(K) = \lambda_M(K) = 1$, $P^{\mathrm{T}}K = (0.1, 0.2)$. By (8), we have $s_0 = \{\boldsymbol{e} | e_1 + 2e_2 = 0\}$. According to (9), the SMC is set to be

$$\begin{aligned} v(x,t) &= -(2,4)(\Delta \boldsymbol{e} - A\boldsymbol{e} + C\widetilde{\boldsymbol{f}}) - 20\left(\varrho \boldsymbol{S} + \varepsilon \frac{\boldsymbol{S}}{\|\boldsymbol{S}\|}\right) \\ &= -2\Delta e_1 - 4\Delta e_2 - 12e_1 - 4e_2 - 20\frac{e_1 + 2e_2}{\|e_1 + 2e_2\|} \\ &\quad - \big(\tanh(u_d^1) - \tanh(u_1)\big) + 0.4\big(\tanh(u_d^2) - \tanh(u_2)\big) \\ &\quad + 10\big(\tanh(u_d^1) - \tanh(u_1)\big) + \tanh\big(u_d^2\big) - \tanh(u_2), \end{aligned}$$

where $\boldsymbol{S} = e_1 + 2e_2$. $\varepsilon = 1$ is used in the simulation.

Other parameters are given as $KP = (0.1, 0.2)^{\mathrm{T}}$, $P^{\mathrm{T}}KP = 0.05$, $KPP^{\mathrm{T}}K = 0.05$. Then $\widetilde{B} = (P^{\mathrm{T}}KP)^{-1}P^{\mathrm{T}}K = (2,4)$, $B = P\widetilde{B} = \left[\begin{smallmatrix} 0.2 & 0.4 \\ 0.4 & 0.8 \end{smallmatrix}\right]$, $X = E - B = \left[\begin{smallmatrix} 0.8 & -0.4 \\ -0.4 & 0.2 \end{smallmatrix}\right]$. Since $\alpha = \beta = 1$ is chosen in this example, then $\widetilde{K} = K$ is the semipositive definite matrix. $XC = \left[\begin{smallmatrix} 0.5 & -0.2 \\ -5 & 0.5 \end{smallmatrix}\right]$, $\|KC\|_F = 4.0311$.

This means that $\gamma - n\gamma^{-1}\|KC\|_F^2\|\Sigma\tilde{Q}\|_F^2 = 0.3126 > 0$. So (H4) is fulfilled.

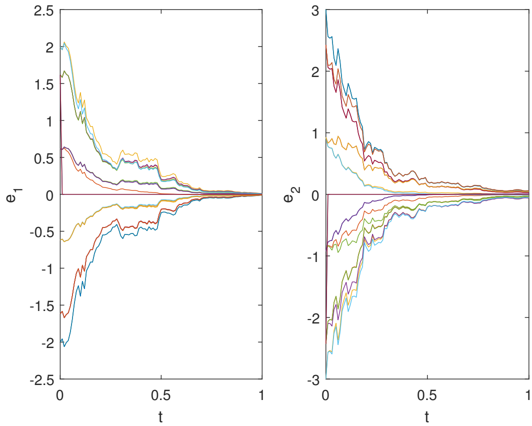

Figure 3. Frequency of e_1 and e_2 in error system without control.

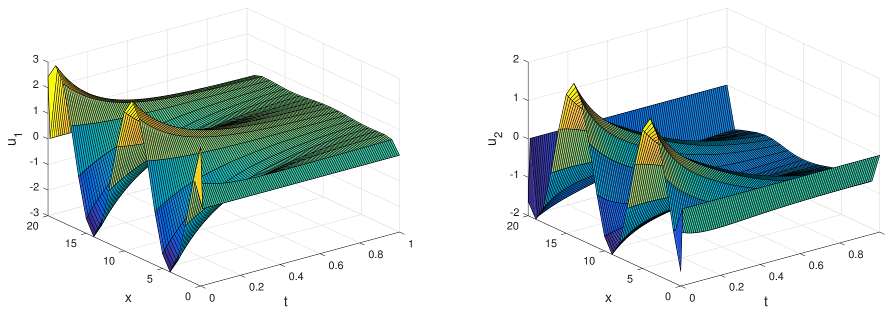

(a) (b)

Figure 4. Dynamical behavior of e_1 and e_2 under SMC.

With these conditions discussed above, the behavior of (17) and (18) is exponentially synchronized under (9) in the mean-square sense by Theorem 1. The results can be validated through the simulation results; see Figs. 4(a), 4(b).

We can see that as time t increases to the infinity, the error surfaces of e_1 and e_2 converge to the equilibrium $\mathbf{0}$ in the sliding mode. The surface is much smoother than that of error system without control, and the impact of random noise is much smaller than that in the open loop system, although the scattering still exists in the controlled system. It coincides with the result of Theorem 1.

6 Conclusion and discussion

The synchronization of delayed SRDHNNs has been solved by using SMC. The result is also validated through an example with simulation. The main theoretical innovation is the construction of switching control law. The construction is novel, and there is no similar work until yet.

The work can be improved further in the following ways. To begin with, integral switching surface is suggested to replace the linear switching surface in the next work. Second, the decomposing method is used to deduce the asymptotic behavior of switching surface of SRDHNNs with s-delays. Third, equivalent control is a sophisticated method in designing the controller, but we still do not know how to construct the appropriate equivalent control for the SRDHNNs with s-delays. We even do not know whether it exists or not for stochastic system. It will be a great challenge for us. The design of switching is very tricky, and it depends on the control gains P. We hope this constraint can be removed in the next article. The controller can also be improved in some sense.

Furthermore, the criteria are described explicitly and given in the form of matrix norm in this work, but some scholars and engineers prefer to use the criteria based on linear matrix inequalities (LMIs) form [2, 3, 16, 26], which can be formulated as convex optimization problems. It is also easy to check since there is a LMIs toolbox in Matlab. This is our another research direction in the future.

Leakage delay effect is missed in this paper, but it plays a more and more important role in the HNNs as convinced by Prof. Cao's team [1, 15]. Moreover, if the mean value of the random process is not zero, how will the synchronization property of the system be affected? This is another interesting topic. Practical applications of SRDHNNs with s-delays is not considered in this article. The recent progress of HNNs shows that image encryption is potential area of application of SRDHNNs with s-delays [20, 21]. We will deal with it in the subsequent work.

Conflicts of interest. The authors declare no conflicts of interest.

Acknowledgment. We sincerely acknowledge the distinguished and rigorous reviewers for their invaluable comments and professional advice. The paper is significantly improved through their suggestions. We would also like to appreciate the serious editors for their selfless help. The article could not have been published without their conscientious work.

References

1. Y. Cao, S. Ramajayam, R. Sriraman, R. Samidurai, Leakage delay on stabilization of finite-time complex-valued BAM neural network: Decomposition approach, *Neurocomputing*, **463**(C): 505–513, 2022, https://doi.org/10.1016/j.neucom.2021.08.056.

2. W. Chen, Z. Guan, X. Lu, Delay-dependent exponential stability of uncertain stochastic systems with multiple delays: An LMI approach, *Syst. Control Lett.*, **54**(6):547–555, 2005, https://doi.org/10.1016/j.sysconle.2004.10.005.

3. M. Forti, A. Tesi, New conditions for global stability of neural networks with application to linear and quadratic programming problems, *IEEE Trans. Circuits Syst., I, Fundam. Theory Appl.*, **42**(7):354–366, 1995, https://doi.org/10.1109/81.401145.

4. Q. Gan, Exponential synchronization of stochastic Cohen-Grossberg neural networks with mixed time-varying delays and reaction-diffusion via periodically intermittent control, *Neural Netw.*, **31**(6):12–21, 2012, https://doi.org/10.1016/j.neunet.2012.02.039.
5. H. Huang, G. Feng, Synchronization of nonidentical chaotic neural networks with time delays, *Neural Netw.*, **22**(7):869–874, 2009, https://doi.org/10.1016/j.neunet.2009.06.009.
6. L. Huang, X. Mao, SMC design for robust H^∞ control of uncertain stochastic delay systems, *Automatica*, **46**(2):405–412, 2010, https://doi.org/10.1016/j.automatica.2009.11.013.
7. X. Liang, L. Wang, Y. Liu, Sliding mode control for Hopfield neural networks with time-delays and reaction-diffusion terms, *Control Theory Appl.*, **29**(1):47–52, 2012, https://kns.cnki.net/kcms/detail/44.1240.TP.20120227.1342.019.html.
8. X. Liang, L. Wang, Y. Wang, R. Wang, Dynamical behavior of delayed reaction–diffusion Hopfield neural networks driven by infinite dimensional Wiener processes, *IEEE Trans. Neural Netw. Learn. Syst.*, **27**(9):1231–1242, 2016, https://doi.org/10.1109/tnnls.2015.2460117.
9. X. Liang, S. Wang, R. Wang, X. Hu, Z. Wang, Synchronization of reaction–diffusion Hopfield neural networks with s-delays through sliding mode control, *Nonlinear Anal. Model. Control*, **32**(2):331–349, 2022, https://doi.org/10.15388/namc.2022.27.25388.
10. X. Liu, K. Zhang, W.-C. Xie, Pinning impulsive synchronization of reaction–diffusion neural networks with time-varying delays, *IEEE Trans. Neural Netw. Learn. Syst.*, **28**(5):1055–1067, 2017, https://doi.org/10.1109/TNNLS.2016.2518479.
11. B. Lu, H. Jiang, C. Hu, A. Abdurahman, Synchronization of hybrid coupled reaction–diffusion neural networks with time delays via generalized intermittent control with spacial sampled-data, *Neural Netw.*, **105**:75–87, 2018, https://doi.org/10.1016/j.neunet.2018.04.017.
12. Q. Luo, F. Deng, J. Bao, B. Zhao, Sliding mode control for a class of Itô type distributed parameter systems with delay, *Acta Math. Sci.*, **27**(1):67–76, 2007, https://doi.org/10.1016/S0252-9602(07)60006-X.
13. H. Lütkepohl, *Handbook of Matrices*, John Wiley and Sons, Chester, 1996, https://doi.org/10.1017/S0266466698143086.
14. Q. Ma, S. Xu, Y. Zou, G. Shi, Synchronization of stochastic chaotic neural networks with reaction-diffusion terms, *Nonlinear Dyn.*, **67**(3):2183–2196, 2012, https://doi.org/10.1007/s11071-011-0138-8.
15. R. Manivannan, Y. Cao, K.T. Chong, Unified dissipativity state estimation for delayed generalized impulsive neural networks with leakage delay effects, *Knowledge-Based Syst.*, **254**(7):109630, 2022, https://doi.org/10.1016/j.knosys.2022.109630.
16. A.N. Michel, D. Liu, *Qualitative Analysis and Synthesis of Recurrent Neural Networks*, CRC Press, Boca Raton, FL, 2018, https://doi.org/10.1201/9781482275780.
17. Y. Niu, D.W.C. Ho, J. Lam, Robust integral sliding mode control for uncertain stochastic systems with time-varying delay, *Automatica*, **41**(5):873–880, 2005, https://doi.org/10.1016/j.automatica.2004.11.035.
18. L. Pecora, T. Carroll, Synchronization in chaotic systems, *Phys. Rev. Lett.*, **64**(8):821–824, 1990, https://doi.org/10.1103/PhysRevLett.64.821.

19. Y. Sheng, Z. Zeng, Impulsive synchronization of stochastic reaction–diffusion neural networks with mixed time delays, *Neural Netw.*, **103**:83–93, 2018, `https://doi.org/10.1016/j.neunet.2018.03.010`.
20. M.T. Thendral, T.R.G. Babu, A. Chandrasekar, Y. Cao, Synchronization of Markovian jump neural networks for sampled data control systems with additive delay components: Analysis of image encryption technique, *Math. Methods Appl. Sci.*, 2022, `https://doi.org/10.1002/mma.8774`.
21. T. Wei, P. Lin, Q. Zhu, Q. Yao, Instability of impulsive stochastic systems with application to image encryption, *Appl. Math. Comput.*, **402**(1):126098, 2021, `https://doi.org/10.1016/j.amc.2021.126098`.
22. L. Wu, D.W.C. Ho, Sliding mode control of singular stochastic hybrid systems, *Automatica*, **46**(4):779–783, 2010, `https://doi.org/10.1016/j.automatica.2010.01.010`.
23. W. Wu, T. Chen, Global synchronization criteria of linearly coupled neural network systems with time-varying coupling, *IEEE Trans. Neural Netw. Learn. Syst.*, **19**(2):319–332, 2008, `https://doi.org/10.1109/TNN.2007.908639`.
24. X. Yan, J. Cao, Z. Yang, Synchronization of coupled reaction-diffusion neural networks with time-varying delays via pinning-impulsive controller, *SIAM J. Control Optim.*, **28**(5):3486–3510, 2013, `https://doi.org/10.1137/120897341`.
25. X. Yang, J. Cao, J. Liang, Exponential synchronization of memristive neural networks with delays: Interval matrix method, *IEEE Trans. Neural Netw. Learn. Syst.*, **28**(8):1878–1888, 2017, `https://doi.org/10.1109/TNNLS.2016.2561298`.
26. D. Yue, Q.-L. Han, Delay-dependent exponential stability of stochastic systems with time-varying delay, and Markovian switching, *IEEE Trans. Autom. Control*, **50**(2):217–222, 2005, `https://doi.org/10.1109/TAC.2004.841935`.
27. B. Zhang, F. Deng, S. Xie, S. Luo, Exponential synchronization of stochastic time-delayed memristor-based neural networks via distributed impulsive control, *Neurocomputing*, **286**: 41–50, 2018, `https://doi.org/10.1016/j.neucom.2018.01.051`.
28. J. Zhou, S. Xu, B. Zhang, Y. Zhou, H. Shen, Robust exponential stability of uncertain stochastic neural networks with distributed delays and reaction-diffusions, *IEEE Trans. Neural Netw. Learn. Syst.*, **23**(9):1407–1416, 2012, `https://doi.org/10.1109/TNNLS.2012.2203360`.
29. W. Zhou, D. Tong, Y. Gao, C. Ji, H. Su, Mode and delay-dependent adaptive exponential synchronization in pth moment for stochastic delayed neural networks with markovian switching, *IEEE Trans. Neural Netw.*, **23**(4):662–668, 2012, `https://doi.org/10.1109/TNNLS.2011.2179556`.
30. Q. Zhu, J. Cao, Stability of Markovian jump neural networks with impulse control and time varying delays, *Nonlinear Anal., Real World Appl.*, **13**(5):2259–2270, 2012, `https://doi.org/10.1016/j.nonrwa.2012.01.021`.